

Comparison of ZHAireS and CoREAS radio emission simulations in the Ultra-High Frequency Band

VIATCHESLAV BUGAEV¹, BRIAN RAUCH¹, ROBERT BINNS¹, MARTIN ISRAEL¹ KONSTANTIN BELOV², TIM HUEGE³, JOE LAM², ANDREW ROMERO-WOLF⁴, STEPHANIE WISSEL² AND THE ANITA COLLABORATION.

¹ Department of Physics and McDonnell Center for the Space Sciences, Washington University in St. Louis

² Department of Physics and Astronomy, UCLA

³ Karlsruher Institut für Technologie, Institut für Kernphysik, Campus Nord, D-76021 Karlsruhe, Germany

⁴ Jet Propulsion Laboratory, California Institute of Technology

bugaev@wuphys.wustl.edu

Abstract: The third flight of the high-altitude balloon-borne ANtarctic Impulsive Transient Antenna (ANITA III) planned for December 2014 will be optimized for the measurement of impulsive radio signals from Ultra-High Energy Cosmic Rays (UHE CR), i.e. charged particles with energies above 10^{19} eV, in addition to the high-energy neutrinos ANITA was originally designed for. The event reconstruction algorithm for UHE CR relies on the detection of radio emissions in the frequency range 200-1200 MHz (RF) produced by the charged component of extensive air showers initiated by these particles. UHE CR energy reconstruction methods are based on Monte Carlo simulations of the RF emission from these showers and on modeling of the detector response to such emission. A full UHE CR energy reconstruction algorithm for ANITA III involving detector modeling is a work in progress. In this paper, we evaluate expected systematic uncertainties in ANITA reconstructed energies *only* due to differences in the RF emission models by comparing outputs of two RF simulation packages, CoREAS and ZHAireS, and propagating the differences in the outputs through an energy reconstruction method using an idealized detector model.

Keywords: UHECR, ANITA, energy reconstruction, ZHAireS, CoREAS

1 Introduction

ANITA is a radio detector designed to observe ultra-high-energy cosmic neutrinos [1]. An ultra-high energy neutrino interaction in ice will emit a radio pulse due to the so-called Askaryan effect. In the case of a neutrino skimming the ice, the radio pulse can refract through the ice and be detected from above. Flying some 37 km above the Antarctic ice, the ANITA detector is sensitive enough to pick up weak radio pulses from hundreds of kilometers away and to reconstruct their event locations.

The ANITA prototype flew piggyback with the TIGER instrument in the 2003–04 Antarctic season, followed by the ANITA I flight in 2006–07 and the ANITA II flight in 2008–09. Based on these two flights, an upper limit on the flux of ultra-high energy neutrinos was published in [2].

The neutrino signal at ANITA is expected to have a vertical polarization. However, 16 horizontally polarized events were identified in the ANITA I data, see Fig. 1. These events cannot be associated with ultra-high energy neutrino interactions, and are consistent with the geosynchrotron mechanism of radio emission caused by UHE CRs [3]. The third ANITA flight scheduled for the 2014–15 Antarctic season will be optimized to study UHE CRs.

The modeling of the RF and the ANITA detector explaining the observed event statistics is a work in progress. The goal of the present study is evaluation of systematic uncertainties in energy reconstruction *only* due to discrepancies in electric fields predicted by different RF simulation codes. Therefore, the term “systematic uncertainty of energy reconstruction” used in this paper is actually a systematic uncertainty of energy reconstruction in a hypothetical situation when the differences in RF models of simulation packages

is the only source of systematic errors. We propagate the observed discrepancies in the output of RF simulation packages through an energy reconstruction algorithm using an *idealized* detector model assuming, in particular, the ability to precisely reconstruct the RF power spectrum.

The UHE CR energy reconstruction method for ANITA will be based on look-up tables of RF emission for different combinations of azimuth and zenith angles of CR shower axis for different inclinations and declinations of the Earth’s magnetic field. This combination of parameters will be referred to as *the event geometry*. These tables are being created by Monte Carlo simulations of RF emission from the charged component of CR - induced showers, and they are subject to systematic uncertainties introduced by models used in the packages simulating the showers and radio emission. With enough statistics of simulated events, a comprehensive systematic error analysis will be based on energy reconstruction of events simulated with the ZHAireS simulation package with tables computed by the CoREAS simulation package and vice versa. CoREAS [4] is a plug-in for CORSIKA [5]. ZHAireS [3] is a plug-in for Aires [6].

At the moment, we cannot use the described procedure due to small ZHAireS event statistics, and thus we limit ourselves to a rather qualitative analysis. With this approach we obtain an *upper limit* on the systematic error due to differences in the simulation codes for a chosen event geometry described in section 2. For seven different energies in the interval from 2×10^{19} to 5×10^{20} eV we compared RF from two showers simulated by ZHAireS and CoREAS for the chosen event geometry. Since shower development is a random process, the observed discrepancies should partly

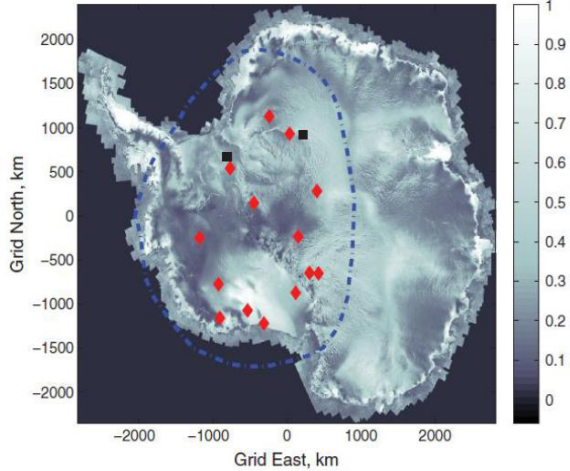


Figure 1: Map of locations of detected reflected (red diamond) and direct (black square) UHE CR events superimposed on a microwave backscatter amplitude map of Antarctica (Radarsat) within ANITA field of view (dash-dotted line) [7]. For the direct events the closest approach to the surface of the RF signals is shown. The scale on the right is relative amplitude of the backscatter signal.

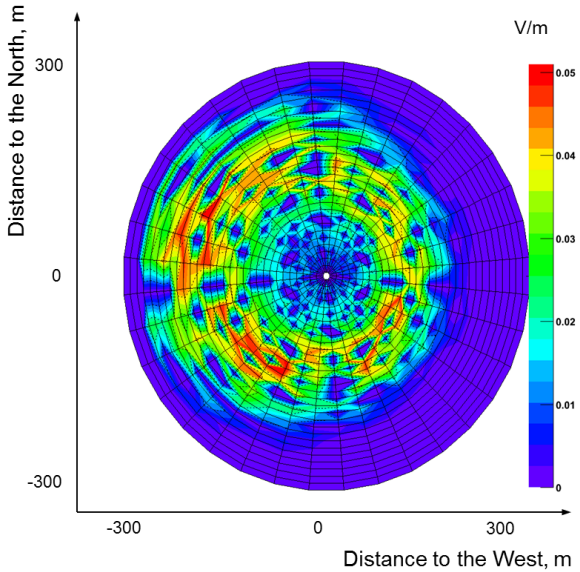


Figure 3: Horizontal polarization component of the electric field on the ice surface at the time of maximum electric field magnitude for one of the ANITA events [8].

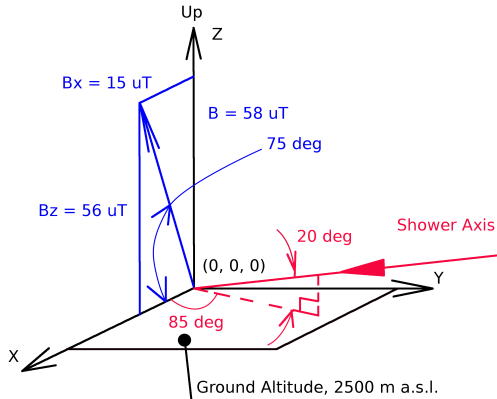


Figure 2: Geometry of the simulated events.

result from fluctuations of shower parameters, especially shower maximum, and differences in maxima of the compared showers may be the main reason for the observed discrepancies in the RF emissions predicted by the simulation packages.

2 Event geometry

Ideally, energy reconstruction for each of the detected events shown in Fig. 1 needs its own set of simulations made for their respective geometries. This will eventually be done for all 16 events, but for this paper we chose one particular event with the geometry shown in Fig. 2. We use this geometry for all plots comparing ZHAireS and CoREAS. All antennas are located along the X axis; we do not consider any other locations. The origin (0,0,0) of the reference frame is defined as the point of intersection of shower axis and the horizontal plane at an altitude of 2500

m above sea level. We refer to it as *the shower core*. The distance from an antenna to the shower core is thus its X coordinate.

The X axis is aligned with the horizontal component of the magnetic field, which is almost vertical. The shower axis is significantly inclined (20°) and is almost perpendicular to the X axis. The RF signal from the shower is developing in the direction of decreasing antenna distances from the shower core.

3 Signal on the ground

Ultimately, we want to estimate the energy of a CR given the signal from the shower detected at the payload, which in most cases will probably be reflected from the ice. In this paper we focus on comparing RF signals on the ground in order to assess systematic errors in energy reconstruction related to differences in RF models. We use the assumption that discrepancies in RF due to the simulations observed at the ground are the same as at the payload, and that an energy reconstruction algorithm based on look-up tables built for the payload is as sensitive to the discrepancies as a method reconstructing energies for a detector on the ground.

For an index of refraction greater than one, the radio emission from a shower form a ring-like pattern on the ice surface similar to one created by Cherenkov emission. For that reason, we will call such a pattern *Cherenkov ring*. An example of a ring-like pattern is presented in a simulation of an ANITA event shown in Fig. 3. The purpose of this plot is to illustrate the concept of a Cherenkov ring to which we will be referring later. The corresponding event geometry is different from the one that was chosen for comparison of the simulation packages, but the ring structure is representative.

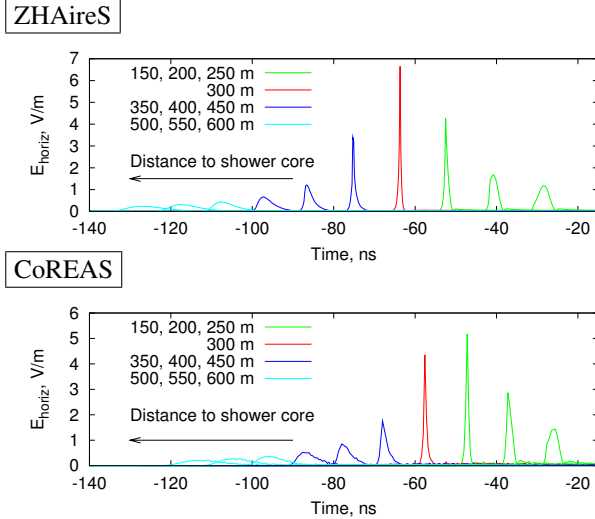


Figure 4: Time series for horizontal component of electric field on the ground. Different locations of antennas are compared for ZHAireS and CoREAS simulation codes.

4 Results

4.1 Time series

Radio pulses from showers with a primary particle energy of 5×10^{20} eV are shown in Fig. 4 for antennas located from 150 to 600 m from shower core in 50 m steps. Results from both ZHAireS and CoREAS are presented. The origin of time $t = 0$ is fixed at the moment at which the shower front reaches ground. The shower azimuth is 275° , i.e., the shower comes from the direction almost perpendicular to the axis on which antennas are located. The shower develops from larger to smaller antenna coordinate values. This makes it possible for RF signals to arrive earlier at antennas located farther away from the shower core. The arrow in the plots shows that the distance from the shower core increases for the peaks that are more to the left. A Cherenkov ring with the width of $\simeq 150$ m can be seen in the data, and a clear maximum in the pulse amplitudes can be identified for the antenna at 300 m (red line) in the ZHAireS panel and at 250 m in the CoREAS panel. This maximum corresponds to an imaginary circle passing through the red area inside the Cherenkov ring in Fig. 3, and we will refer to this circle as the *middle* of Cherenkov ring.

We found that for CoREAS the middle would be found in an interval closer to shower core. The difference in the locations of the middle of Cherenkov rings for the two codes could possibly be a result of comparing showers with different shower maxima, although with our limited statistics we did not find such a correlation. Also, the showers shown in Fig. 4 have maxima at the same depth to within 1 g/cm^2 , which suggests that the middle of the Cherenkov ring is systematically shifted for one simulation code compared to the other, probably due to a difference in the refraction index model.

4.2 Frequencies

Frequency distributions are compared in Fig. 5 for CoREAS and ZHAireS RF simulation packages using the same 5×10^{20} eV showers as in Fig. 4, which means that the shower maxima are the same. Fourier transforms are shown for both CoREAS (thin lines) and ZHAireS (thick lines), where different colors represent different components of

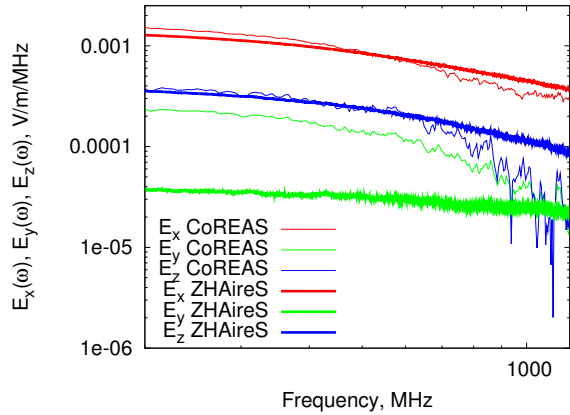


Figure 5: Comparison of frequency distributions based on data simulated with CoREAS and ZHAireS RF simulation packages. Electric fields are considered in the middle of their Cherenkov rings (300 m from the shower core for ZHAireS, 250 m for CoREAS). $E = 5 \times 10^{20}$ eV.

the electric field (x, y, z). The horizontal component of the electric field is seen to dominate, which is expected for the geometry of our event. In our particular case the differences between horizontal components are determined by the x-component of electric field (red curves).

The electric fields shown are those for the middle of their respective Cherenkov rings. In particular, for events in Fig. 5, ZHAireS distributions are taken for the antenna at 300 m from shower core, while for CoREAS the analogous distance is 250 m. In order to compare frequency distributions for other energies, we took each distribution from the middle of the Cherenkov ring of the corresponding shower, similarly to what we did to compare frequency distributions in Fig. 5. We found that the discrepancies in x components do not exceed $\simeq 30\%$ near 200 MHz, i.e. the lower bound of ANITA's sensitivity. Discrepancies tend to be larger for higher frequencies and are a factor of $\simeq 2$ near the 1200 MHz upper bound of ANITA's sensitivity. A rather coarse 50 m precision with which the middle of the Cherenkov ring is determined is one of the possible reasons for making the observed discrepancies larger than they actually are. We ignore the blue line since for the given configuration the contribution of the y component to horizontal polarization is negligible. At the same time, discrepancies in blue and especially green lines show substantial differences in RF models used in CoREAS and ZHAireS.

Power spectrum density scales as square of frequency distribution. Therefore the discrepancies between frequency distributions at 200 and 1200 MHz determine the interval for systematic uncertainty for the predicted total power in the ANITA frequency band, which is a factor of 1.7 – 4. Knowing that the higher frequency end contributes more to the uncertainty, an energy reconstruction algorithm can be optimized by lowering the upper bound of the interval used to compute the total power. Based on frequency distributions similar to those presented in Fig. 5, we computed the total power P of the electric field horizontal component in 200 MHz – 1200 MHz band for different energies E^i on a grid with the step size $\log_{10} E^{i+1} - \log_{10} E^i \equiv \Delta \log_{10} E = 1/10$. The total power as function of distance from shower core is presented in Fig. 6 for different energies. For readability, we do not show curves for all energies E^i , but only for a

